

Investigating the Relationship between Adhesion Forces and Surface Functionalization Using Atomic Force Microscopy

Mikhail Trought and Kathryn A. Perrine*



Cite This: *J. Chem. Educ.* 2021, 98, 1768–1775



Read Online

ACCESS |

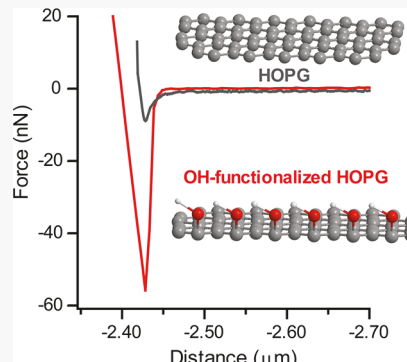
Metrics & More

Article Recommendations

Supporting Information

ABSTRACT: Surface chemistry impacts technology, advancing the development of new heterogeneous catalysts, semiconductor devices, and materials synthesis. Carbon surfaces are ubiquitous in various fields, and the surface reactivity can be altered by surface functionalization on the molecular scale, introducing functional groups, thus shifting their macroscale properties. In this physical chemistry lab experiment, students use atomic force microscopy to investigate the surface of graphite (organic) and gold (inorganic) samples (solid phase) to compare topographical features, surface roughness, and adhesion forces of the samples. Students relate the force–displacement measurements with the Lennard-Jones potential to obtain measurable adhesion forces. Emphasis is placed on quantification of the adhesion forces between a hydrophobic highly oriented pyrolytic graphite (HOPG) surface, a hydrophilic (hydroxy) functionalized HOPG surface, and a metallic gold-coated glass slide. The surface of each sample is explored, allowing students to compare the difference between the hydrophobic and hydrophilic surfaces from surface functionalization.

KEYWORDS: Upper-Division Undergraduate, Analytical Chemistry, Physical Chemistry, Hands-On Learning/Manipulatives, Materials Science, Nanotechnology, Surface Science



INTRODUCTION

Impact of Atomic Force Microscopy on Surface Science, Technologies, And Education

Atomic force microscopy (AFM) is an essential instrument that is used to measure the three-dimensional topography of surfaces at the nanoscale. This invaluable surface technique continues to impact technological developments in the semiconductor industry, heterogeneous catalysts that drive clean energy production, bioinspired materials for self-adhesion, solar cells, wearable sensors, and environmental cleanup.^{1,2} In education, real-time imaging amazes students of all ages allowing them “to see” the surface of materials that are more than 1000 times smaller than a human hair.³ One of the key goals in the chemistry curriculum is for students to relate the changes on the molecular scale with macroscale properties of materials, emphasizing macromolecular chemistry, nanoscience, and even material science concepts, connecting structure–property relationships.^{4,5} The interdisciplinary field of surface science merges organic, inorganic, and physical chemistry impacting students from the chemistry, physics, biology, and engineering disciplines. These fields encourage students to learn and relate physical and chemical properties at the nanoscale through hands-on learning activities. These types of undergraduate laboratory experiments provide undergraduate students with opportunities to solve real-world research problems and connect them to fundamental physical chemistry concepts.^{6–8}

Several excellent studies and student laboratory experiments have utilized AFM to investigate the topography of materials at the nanoscale.^{9–12} However, there are few undergraduate experiments that implement surface chemistry, such as surface modification by (bottom-up) functionalization, with surface science investigations. These studies are important for connecting nanoscale topographical features or surface functional groups, with properties of the material on the macroscale.¹³ Surface functionalization plays a vital role in the development of semiconductor devices, heterogeneous catalysts, battery research, and biobased materials, where molecular functionalization directs growth of materials to specific sites impacting device performance. Surface functionalization can be used for area selective atomic layer deposition as it provides a way to use functional groups (active sites) for growth of metal or metal oxide nanoparticles and films that are currently being realized for semiconductors and catalyst design processes.^{14,15} This laboratory experiment provides students with the opportunity to investigate the effects of surface functionalization.

Received: June 2, 2020

Revised: March 5, 2021

Published: March 30, 2021



Surface functionalization can be implemented on carbon-based materials. Graphene-based technologies and other 2D materials are intensely investigated as potential new materials in the aforementioned fields of semiconductor design and catalysis, as well as in the broad field of nanotechnology.^{13,16–18} Highly oriented pyrolytic graphite (HOPG) has been used in the field of surface science as a model graphene surface, due to its sp^2 -hybridized carbon network, ease of preparation, and well-defined surface sites, such as the planar graphene terrace and step-edge defects.¹⁹ Because of its surface structure, HOPG is known to be hydrophobic and air-stable.^{20,21} Additionally, treatment of graphene and related carbon nanomaterials with oxidizers produces graphene oxide of various morphologies.^{17,22} Similar surface treatments can be used to produce (hydroxy) functionalized graphite.²³ The surface oxidation causes the delamination of the graphitic surface by etching away sheets of graphene, resulting in trenches, holes, and various defects in the surface.^{23–25}

In this lab experiment, the surface of HOPG is compared to a hydroxy (OH) functionalized HOPG, produced from etching with nitric acid. In our previous work, we²² and others^{26,27} have observed that HOPG becomes functionalized with OH groups, through surface oxidation, as observed by X-ray photoelectron spectroscopy. We have also observed that when the HOPG surface is exposed to concentrated nitric acid, the surface topography is drastically affected, producing large trenches on the HOPG surface on the nanoscale compared to untreated HOPG.^{22,23} These topographical features and roughness were quantified in this lab experiment in comparison to the flat HOPG surface, the unfunctionalized surface with no oxygen groups, and sputter-deposited gold, a metallic surface that is also unreactive in ambient air. In this study, force-pull measurements (force–displacement curves) are used to quantify the adhesion force, which is defined as how much force is required to pull the tip away from the surface.²⁸ The HOPG surface is functionalized by exposure to nitric acid that produces OH functional groups, which can hydrogen bond with water vapor (in air), as observed for molecules with polar groups.^{22,29} The adhesion forces are quantified for the hydrophobic HOPG and gold surfaces, and the hydrophilic OH-functionalized HOPG surface in comparison with literature values. Students connected the concept of hydrophobic vs hydrophilic forces with the surface functionalization to provide a quantitative measure of the surface changes and the macroscopic observation of adhesion. They also compared and contrasted the surface topography of the HOPG surface, OH-functionalized HOPG surface, and a gold surface.

This lab was developed for our physical chemistry II lab course (quantum chemistry) to address the relationship between intermolecular forces and surface modification. This allows students to not only use state-of-the-art instrumentation to visualize nanoscale features, but also investigate how surface modification by functionalization on the atomic scale affects adhesion forces on a surface. This lab was completed three times in three academic years, by 25 students. Students were assessed by answering questions in their lab report relating the learning goals of the lab to their observations and the data collected, including describing the features on the surface and how the surface roughness relates to the nanoscale topography, comparing and contrasting the force–displacement measurements between the samples with and without functional groups, and explaining the significance of the force–displacement measurements and how they would apply these measurements

on the AFM to other technologies and disciplines. These addressed the following learning goals:

1. recognize the Lennard-Jones potential is a model for the adhesion force measurements between an AFM tip and the surface
2. connect molecular scale functionalization (nanoscale observations) with adhesion force measurements
3. investigate how measurements on the nanoscale influence macroscale properties (hydrophilicity)
4. distinguish the differences between hydrophilic and hydrophobic surfaces

This discovery-based lab emphasizes the importance of surface chemistry in carbon-based technologies that comprise electronic devices and are used as supports for heterogeneous catalysts.^{14,30,31}

■ BACKGROUND OF AFM AND FORCE SPECTROSCOPY

AFM was first invented by Binnig, Quate, and Gerber,³² and consists of a probe (cantilever) with a tip that is nanometers in diameter, which rasters across a surface, collecting a three-dimensional map of the surface. Images of the surface topography are obtained by tracking the deflection of the cantilever due to the interaction of the tip of the cantilever and the features on the surface.³³ Initially, the tip is brought in contact with the surface, where a laser is reflected off of the reflective coating on the backside of the cantilever, and the tip position is detected by a photodiode. Figure 1 shows a schematic representation of a typical AFM setup.

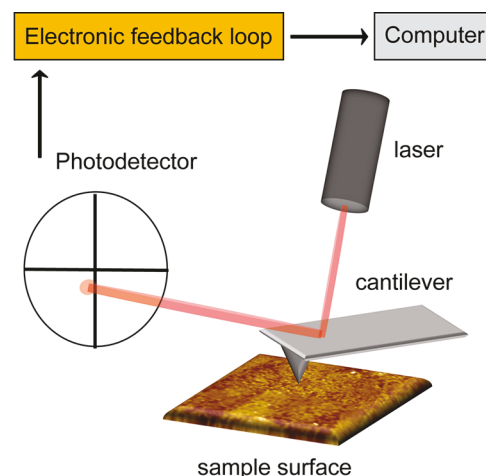


Figure 1. Schematic of the atomic force microscope instrument setup.

Tapping mode, a type of imaging mode, is typically used to collect AFM images in which the cantilever tips are excited at their resonance frequency causing oscillations.³⁴ As a result of this, the tip scans the surface of interest by intermittent contact between the tip of the cantilever and the surface, producing a three-dimensional topographical image of the surface. Force–displacement measurements can be employed to investigate the adhesion forces of the tip interaction with the surface. Force spectroscopy curves are obtained at a defined location on the surface of the sample and can be described simplistically using the Lennard-Jones potential, as shown in Figure 2.^{20,35}

The Lennard-Jones potential describes the interaction of the tip of the cantilever, ideally a single atom, with an atom of a

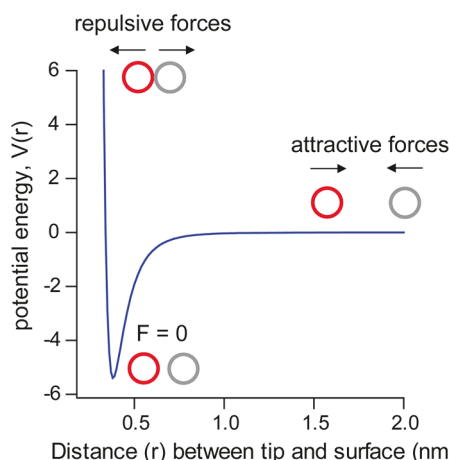


Figure 2. Plot of the Lennard-Jones potential illustrating attractive and repulsive forces between an atom on the tip of the cantilever (gray) and an atom on the surface (red). When the tip of the cantilever and the surface are in close contact, the force between them is at a minimum or the change in potential energy is zero ($F = 0$).

feature on the surface. Force–displacement curves are first collected by allowing the tip of the cantilever to overcome the distance between itself and the sample surface. As the tip moves closer to the surface, it experiences van der Waals attractive forces from the sample's surface.³⁶ When the tip comes in contact with the surface, electrostatic repulsion occurs between the tip and the sample. During contact with the surface, there is interaction of the tip and the surface through an adsorbed water layer resulting in capillary forces, which depends on the chemical composition of the surface and the probe, as well as the ambient humidity.³⁷ On retraction of the cantilever, the cantilever bends forcing the tip to overcome the adhesion force associated with its interaction with the surface. This causes the cantilever to pull off sharply toward the probe's equilibrium position, thus representing the depth of the well of the Lennard-Jones potential. In ambient environments, the force–displacement measurement is a combination of van der Waals forces, adhesion forces, and capillary forces.^{36,38} In engineering disciplines, this requires additional theory to measure surface energy, and measurements can depend greatly on relative humidity, the shape of the tip, and the roughness of the surface.^{28,37,39} For our chemistry laboratories, the basic theory was applied for students to measure the adhesion force, comparing these differences between samples, with the relative humidity between 32–48%.

METHODS

Sample Preparation

A watch glass and a glass pipet were cleaned prior to the experiment by soaking the pipet in concentrated nitric acid (HNO_3) (70% fuming nitric acid, Aldrich) for 2 h to remove organic contamination. The glassware was rinsed with ultrapure water (18 $\text{M}\Omega\text{-cm}$ resistivity, Millipore Sigma) and air-dried. HOPG was prepared by cross sectioning the 10 mm \times 10 mm samples (ZYB grade, MikroMasch USA) in half to produce 5 mm \times 10 mm sizes. The surface of the HOPG samples were then cleaved using the adhesive tape exfoliation method to remove uneven layers to produce a flat sample with a mirror-like finish. The OH-functionalized HOPG surface was prepared by dropping concentrated (15.8 M) HNO_3 onto the HOPG surface to form a droplet, using the glass pipet in a ventilated

fume hood. (Figure S1 shows an example of the HOPG sample during the acid etching process in the instructors notes in the [Supporting Information](#).) The surface was acid etched (oxidized) for 2 h and immediately rinsed with 50 mL of ultrapure water. After rinsing, the sample was placed on a Kimwipe to dry in air. All samples were mounted on a glass slide, previously cleaned with ethanol, using carbon tape (Ted Pella, Inc.) for AFM imaging.

The gold sample was prepared by first cleaning a glass slide by washing with diluted Micrell soap solution and water. The slide was then soaked in nitric acid as described above. After drying, the glass slide was coated with 5 nm of chromium followed by 120 nm of gold (Au) using the PerkinElmer 2400 sputter system in the Microfabrication Facility at Michigan Technological University. Gold-coated slides are commercially available for purchase from Ted Pella, Inc. or similar company. The sputter deposition technique typically produces a rougher film than using an etched gold foil or a gold single crystal. Either type of gold surface is sufficient for the adhesion force measurements but may produce different surface roughness values. Prior to imaging, samples were rinsed with ethanol and air-dried. It is important to not use any material to wipe the surfaces of the samples prior to imaging. This will result in dust fibers on the samples producing anomalous features or alter the hydroxy (OH)-functionalized HOPG surface. Also note that the OH-functionalized HOPG can be prepared up to 1–2 days ahead of time and stored in a dust-free environment.

AFM Measurements (Topography and Force Curves)

The students collected images, surface roughness measurements, and force curves using an AFM instrument. An Asylum Research MFP-3D Origin atomic force microscope was used to collect all data with a monolithic silicon aluminum-coated AFM cantilever with a force constant 40 N/m and frequency of 300 kHz (Budget Sensors) to image all samples using tapping mode (AC mode). AFM images of sizes 20 $\mu\text{m} \times 20 \mu\text{m}$, 10 $\mu\text{m} \times 10 \mu\text{m}$, and then 2.3 $\mu\text{m} \times 2.3 \mu\text{m}$ were collected on all surfaces at a scan rate of 1.0 Hz with 256 points per line. All images were processed using third-order flattening. Surface roughness of all surfaces were investigated using root-mean-square (RMS) roughness values collected using a 400 nm \times 400 nm area, that was placed at different locations on a 2.3 $\mu\text{m} \times 2.3 \mu\text{m}$ image. The RMS roughness is the root-mean-square of the vertical deviation from the plane of the surface and is sensitive to variation in surface height. Either the average roughness (typically denoted Ra) or the RMS could be used, as they are related. The smallest sized images (2.3 $\mu\text{m} \times 2.3 \mu\text{m}$) were used to collect RMS roughness values using 256 points per line, as it had the highest resolution. The RMS roughness values will vary on larger sized areas, such as the 20 $\mu\text{m} \times 20 \mu\text{m}$ area, as larger distances between the points are collected, and may incorporate larger deviations of height than smaller sized areas. The RMS roughness measurements were done using the Asylum Research software. This postprocess analysis can be applied using free software, as described in the [Supporting Information](#). The students were introduced to various parameters of the software and were given demonstrations. Students utilized the software functions to obtain AFM images and the RMS roughness values. Averages and standard deviations were computed from the collected data. Instructions on these features of the software are given in the [student instruction handout](#) and the [raw RMS values](#) are given in the [Supporting Information](#).

Adhesion forces were measured by collecting force displacement curves. The force displacement curves were obtained from a single point of interest using the Asylum Research software. At the beginning of the force–displacement measurement, the tip of the cantilever, is situated at a location far from the sample. As it approaches the surface, the tip interacts with the surface and experiences attractive and repulsive forces, which causes the tip to move down or up, respectively. When the attractive force of the tip and the sample exceeds that of the spring constant of the cantilever, the tip has made contact with the sample. The AFM cantilever motion is governed by Newtonian mechanics (Hooke's Law), where the spring constant of the cantilever is directly related to the force on the cantilever (F) and the deflection of it (r), as shown in eq 1. The spring constant (k) is dependent upon the physical properties of the cantilever, as described in eq 2.⁴⁰

$$(F = kr) \quad (1)$$

$$\left(k = \frac{Ewt^3}{4l^3} \right) \quad (2)$$

where E is Young's modulus, a measure of the sample stiffness, w is the width, t is the thickness, and l is the length, the dimensions of the cantilever. The adhesion force (in nN) is obtained by multiplying the spring constant (in nN/nm) by the cantilever deflection (nm).^{41,42}

The interaction of the tip with the sample will continue to increase as the tip moves downward until the trigger point is reached (about 100 nN). The trigger point is a value selected by the user, which prompts the piezo to change the direction as part of the measurement. In the imaging mode, the user can select a set point to exert the same force on the samples, so that the adhesion forces can be quantitatively compared. Upon retraction of the tip, the interaction force will decrease as the tip is raised from the sample, with the tip still in contact with the sample, due to the adhesion and capillary forces. The tip will move back to its original position, once it overcomes the attractive force. An illustration of the force–displacement measurement is shown in Figure 3 and in the student instructions.

The force–displacement curves were obtained on $2.3 \mu\text{m} \times 2.3 \mu\text{m}$ sized images. The distance traveled during this measurement was $5 \mu\text{m}$. The cantilever of the AFM tip was allowed to dwell toward the surface for 0.99 s with a sampling rate of 2 kHz. The trigger point of all images was set to a force of 100 nN. The adhesion force value was subsequently obtained by taking the difference between the apex of the retraction section of the force curve and the baseline of the approach. Prior to collecting the curves, the tip should be calibrated^{43–45} to obtain meaningful values to compare with literature. It should be noted that the tip calibration corrects for the deflection (sensitivity) and spring constant, that are specific to each individual cantilever and should be done by the instructor. Adhesion force values are provided for each sample using both the calibrated and uncalibrated cantilevers and it was found that the trends for the samples remain the same. These calibrated values are presented below and are available in the Supporting Information for comparison with the uncalibrated data to illustrate qualitatively that the hydrophilic OH-functionalized HOPG surface has a larger adhesion force compared to the hydrophobic HOPG and gold surfaces.

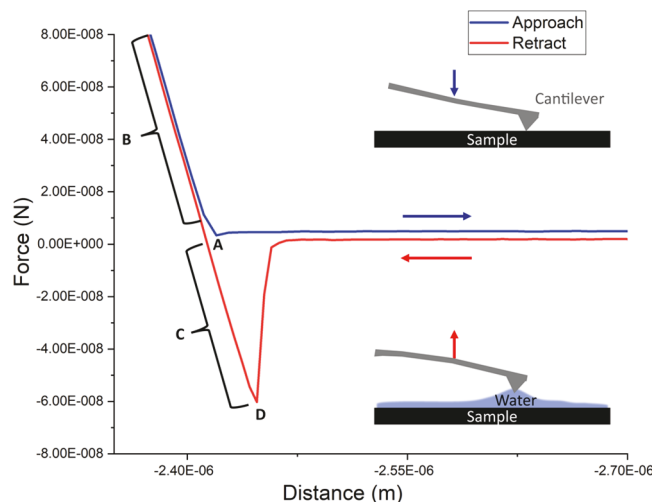


Figure 3. A schematic of the measurement of the force–displacement curve. (A) After approaching the surface, the tip makes contact with the surface. (B) Eventually van der Waals forces set in and the cantilever is then deflected from the surface as it is withdrawn. (C) As the tip retracts from the surface, adhesion and capillary forces from a small amount of adsorbed water hold the tip as it interacts with the surface. The pulling force measured is known as the adhesion force. (D) The probe is then retracted, and the tip is eventually released from the surface region.

All force curves were exported as .csv files in which the students plotted force–displacement curves and used the plots in their final report. Our raw data is in the Supporting Information, which can be utilized for those instructors without an AFM instrument. Students collected three images for each sample, a minimum of three RMS measurements per image, and three force curves over a 4 h period in 1–2 groups. Ideally, if more time is available, students could perform the lab in groups of 2–4 students in a longer time block. This is just enough time to collect all three samples. If imaging of the samples was not ideal during the lab, precollected data were given to students to analyze in their lab report. (The student handout is given in the Supporting Information.) Force–displacement curves were collected on individual points on the AFM image. The RMS measurements were collected using a $400 \text{ nm} \times 400 \text{ nm}$ area box, so even if some features in the entire image were not ideal, the viable areas can be used for a reasonable estimate of the RMS value of the surface. If an AFM instrument is not available, the precollected data, including image files and force–displacement curves, are included in the Supporting Information with suggested access to freely available software.

HAZARDS

It is recommended that the teaching assistants, senior students, or instructors prepare the gold slide and the OH-functionalized HOPG samples, using the procedures described in the sample preparation section. Additional details on the sample preparation for the instructor or senior teaching assistant are given in the Supporting Information. Proper PPE, including gloves and goggles, and caution should be utilized when handling concentrated HNO_3 . The samples were prepared in a well-ventilated hood. The glassware that was used were cleaned and free of any organic carbon contamination to achieve the best results. Nitrile gloves were used when mounting samples for imaging. During scanning, no PPE was worn. Please use COVID-19 protocols at your respective university.

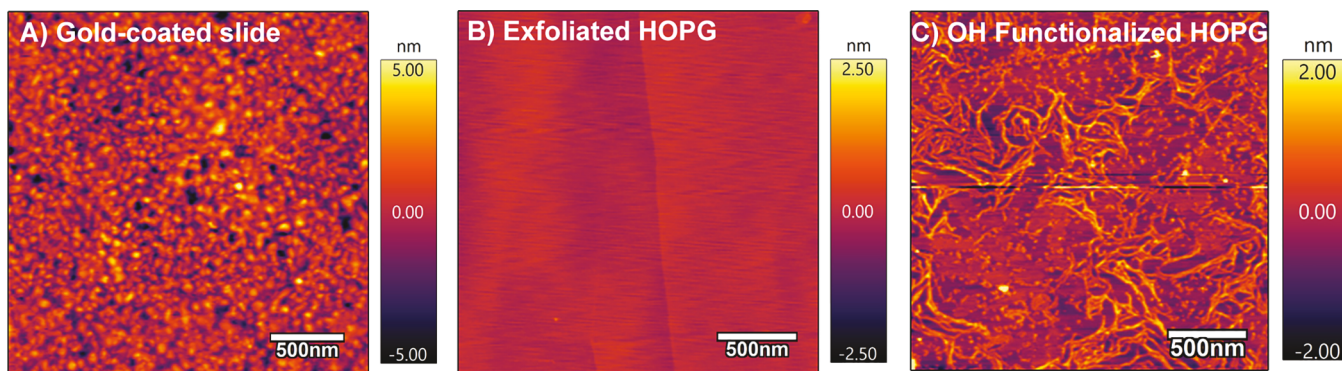


Figure 4. (A) AFM images of the gold-coated glass slide, consists of gold nanosized features that were produced from using the sputter-coating method. (B) The HOPG surface consists of a smooth terrace and a step-edge defect. (C) An OH-functionalized HOPG consists of large trenches and graphitic islands that were produced from the etching the HOPG surface with 15.8 M HNO₃.

RESULTS AND DISCUSSION

AFM Characterization of the Surface Topography of HOPG, OH-Functionalized HOPG and Gold-Coated Glass Slide

AFM images of the gold-coated glass slide, the HOPG, and the OH-functionalized HOPG are presented in Figure 4A–C, respectively. Students made comparisons between features on the surface and the roughness of the surface. The surface of the gold-coated glass slide had a considerably grainy-like surface structure, which appeared to be due to nanoscale Au structures obtained from the sputtering deposition process (Figure 4A). In Figure 4B, a smooth surface is observed with a characteristic step edge on the HOPG surface obtained after exfoliation of the surface with adhesive tape. It is common to observe step-edge defects on the surface of HOPG using AFM. In the OH-functionalized HOPG image (Figure 4C), graphitic islands and trenches are observed to decorate the surface, produced from oxidation with concentrated HNO₃.²³ This shows that when HOPG is exposed to concentrated HNO₃, the surface is oxidized and changes the morphology of the HOPG surface.^{22,23,29,46} It should be noted that Figure 4B shows slight interference in the image, which may have been due to environmental noise and Figure 4C shows an AFM streak, which is an error in the scanning of the image. Streaks are common AFM artifacts and may have occurred due to vibrational noise experienced by the probe during scanning. The students were encouraged to make note of errors observed during scanning and propose possible explanations, to further understand the anomalies of the AFM technique.

Surface Roughness Measurements

The roughness values of the surfaces were determined using the root-mean-square (RMS) as a measure of the variation from the mean of the height. The RMS roughness values and their standard deviation were collected from several spots on different samples, displayed in Table 1. The gold-coated glass slide gave an RMS roughness of 1.19 ± 0.25 nm, which was comparatively the highest RMS roughness value for all the samples. This is mainly due to the deposition process in which a metallic target is

sputtered, removing material to be deposited on the glass slide (substrate) producing a grainy-like film. The HOPG surface had a relatively low roughness value of 0.07 ± 0.02 nm, due to the relatively defect-free graphitic lattice obtained through exfoliation. The HOPG surface treated with 15.8 M HNO₃, had a relatively higher roughness value of 0.58 ± 0.11 nm due to the etching of the HOPG surface, which results in the formation of graphitic islands²⁵ and the unzipping of the top layers of the graphene sheets.^{47,48}

Adhesion Force Measurements

Example force curves associated with each surface showing the force–displacement curve (pull-off force) that were collected from our data are shown in Figure 5A–C. Students collected force curves from various points on the surface and calculated the average and standard deviation for each sample, presented in Table 2. Caution should be taken in selecting the location chosen to collect the force–displacement curves. Force–displacement curves collected on the terrace region could yield the same adhesion force as the unreacted HOPG surface. Additionally, collecting force curves on anomalous features (such as dust, or large step edges) could result in an anomalous adhesion force. The idea is to collect a force curve from a part of the OH-functionalized HOPG surface that is representative of similar features on the oxidized surface. All collected force curves (raw data) are given in the Supporting Information.

Table 2 shows the overall average of the force curves obtained for each of the samples. The HOPG surface had the lowest adhesion force average at 6.39 ± 2.12 nN (uncalibrated tip) and 65.62 ± 19.60 nN (calibrated tip), as expected from a flat graphitic material.^{42,49,50} These values generally agree with those cited in the literature on graphite 13 ± 2 nN,⁴² 25 ± 8 nN,⁴⁹ and graphene (powder) 66.3 nN.⁵⁰ The surface sites expected to interact with the cantilever's tip on graphitic surfaces are the sp² carbon (terrace region) and sp³ carbon (step edges), as well as the thin layer of physisorbed water.^{42,50} Physically adsorbed or physisorbed water is a thin layer of water that is weakly bound (van der Waals forces) to surfaces in ambient conditions. It is well-known that a thin layer of physisorbed water exists on surfaces when exposed to ambient air.^{20,42} Therefore, the relatively low adhesion force maybe due to the occurrence of van der Waals forces and a minor contribution of capillary forces.^{20,36,51} The OH-functionalized HOPG surface produced the largest pull-off force of 57.0 ± 14.3 nN (151.3 ± 37.15 nN for the calibrated tip), due the interaction of water vapor from hydrogen bonding with the OH-functional groups, making it

Table 1. Comparison of Surface Roughness Values

Parameter	RMS (nm) for Each Surface		
	Gold-Coated Glass Slide	HOPG	OH-Functionalized HOPG
av \pm SD	1.19 ± 0.25	0.07 ± 0.02	0.58 ± 0.11

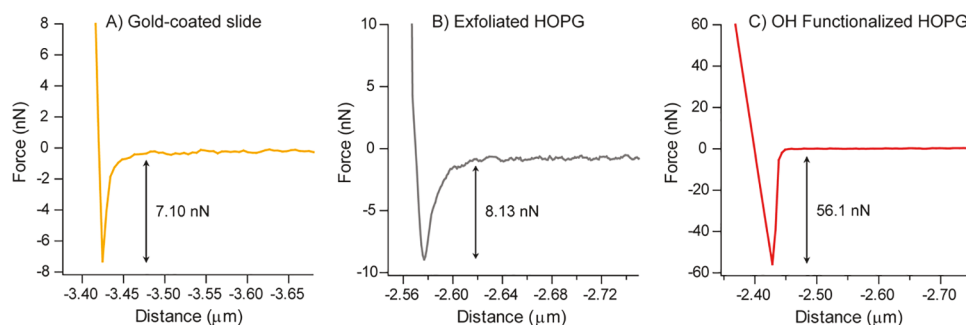


Figure 5. Example force curves of (A) gold-coated glass slide; (B) HOPG; and (C) OH-functionalized HOPG.

Table 2. Comparison of Average Adhesion Force Values of Gold, HOPG, and OH-Functionalized HOPG Surfaces

Parameter	Adhesion Force (nN) for Each Surface					
	Gold-Coated Glass Slide	N	HOPG	N	OH-Functionalized HOPG	N
av \pm SD	7.85 \pm 3.45	30	6.39 \pm 2.12	109	57.0 \pm 14.3	56
av \pm SD (with tip calibration)	127.34 \pm 71.67	96	65.62 \pm 19.60	58	151.3 \pm 37.15	63

comparatively the most hydrophilic surface of the three samples.⁵⁰ These are compared to cited values for graphene oxide (powder), found to be 170.6 nN at 45% relative humidity,⁵⁰ similar to the room conditions for our data. An adhesion force of 7.85 ± 3.45 nN (127.34 ± 71.67 nN for the calibrated tip) for the gold-coated glass slide^{52,53} was higher than that of HOPG, both known to be nonreactive (nonoxidizing) in air. It was expected that the gold surface would have a lower adhesion force, since it is more hydrophobic compared to that of the HOPG surface. This higher measurement is attributed to higher surface roughness, as shown in Figure 2A, due to the deposition process.²⁸ It has been found that the adhesion force for a sputter-deposited gold film is 7.44 nN.⁵² For evaporated gold films, the adhesion force depends on the thickness of the gold film: 91.25 nN (500 nm of gold), 128.5 nN (300 nm of gold), and 212 nN (100 nm of gold).⁵³ The force–displacement measurements are within the error of each other and consistent with previously reported values for gold and HOPG.^{42,49,52} The error was the standard deviation associated with the average of the adhesion force values obtained from the samples.

A presentation was given during the class to help the students connect the concept of the Lennard-Jones potential, in which attractive and repulsive forces are demonstrated in the force–displacement measurements. Students were prompted with questions to address the following concepts and learning goals in their lab reports. In their lab report, they compared and contrasted the topographical features on all three surfaces, with emphasis on how the surface roughness differed between the samples. The adhesion forces were compared from the force–displacement measurements between the hydrophobic HOPG surface, having a low adhesion force, with the hydrophilic OH-functionalized HOPG surface, having a higher adhesion force. The conclusion here is that the physisorbed water layer is present on all the surfaces and it will hydrogen-bond with the OH-functionalized HOPG surface, resulting in the higher adhesion force. This means that it takes more force to pull the tip away from the surface, unlike with the hydrophobic HOPG surface. Students also compared the air-stable surfaces, the gold-coated glass slide to the HOPG surface, to find that the surface of the gold had a higher RMS value, thus resulting in a higher adhesion force. They also discussed potential errors with the image features and roughness, and how those influenced the

force–displacement measurements. Importantly, students were able to show how the knowledge of using the AFM instrument could be used for other applications in different fields and technological developments.

CONCLUSIONS

This lab experiment used AFM to compare the physical and chemical properties of different surfaces for upper level undergraduate students. Students explored concepts such as surface roughness and hydrophobicity of a gold surface, a graphitic (HOPG) surface, and a OH-functionalized HOPG surface. This allowed students to achieve the four learning goals described in the [Introduction](#)

The students were able to observe that the gold sample, prepared by sputter deposition, was a rougher surface compared to the flat HOPG surface and that both produced similar adhesion force measurements. Students observed that the hydrophilic OH-functionalized HOPG surface produced a larger adhesion force and a rougher surface (higher RMS value) compared to the hydrophobic HOPG surface (lower RMS value). This lab provides students experience with investigating the effects of surface functionalization and characterizing materials surfaces on the nanoscale that impact hydrophobic and hydrophilic properties and demonstrates the influence of surface chemistry on designing new materials and devices.

ASSOCIATED CONTENT

Supporting Information

The Supporting Information is available at <https://pubs.acs.org/doi/10.1021/acs.jchemed.0c00558>.

Raw image data files and (JPG) images for each sample (ZIP)

Calibrated adhesionforcevalues; uncalibratedadhesionforcevalues_RMS; calibratedforcedistcurves; uncalibratedforcedistcurves (ZIP)

Notes for instructors (PDF, DOCX)

Student lab handout and instructions (PDF, DOCX)

AUTHOR INFORMATION

Corresponding Author

Kathryn A. Perrine — *Department of Chemistry, Michigan Technological University, Houghton, Michigan 49931, United States; orcid.org/0000-0002-5048-6411; Email: kaperrin@mtu.edu*

Author

Mikhail Trought — *Department of Chemistry, Michigan Technological University, Houghton, Michigan 49931, United States; orcid.org/0000-0003-0705-782X*

Complete contact information is available at:

<https://pubs.acs.org/10.1021/acs.jchemed.0c00558>

Author Contributions

K.A.P. and M.T. cowrote the manuscript. M.T. performed all the AFM measurements, tabulated the data, ran the instrument with the students, and wrote the technical instrument instructions in the student handout. K.A.P. directed the lab experiment, taught the theoretical background to the students, and wrote the student instructions.

Notes

The authors declare no competing financial interest.

ACKNOWLEDGMENTS

Funding from the NSF MRI Grant No. CHE1725818 is acknowledged for supporting the AFM instrument. Sample preparation was supported by the Michigan Technological University 2017 Research Excellence Fund. We also acknowledge the ACMAL facility at Michigan Technological University for access to the AFM instrument. We thank Chito Kendrick for coating the glass slides in the Michigan Technological University Microfabrication Facility.

REFERENCES

- (1) United States National Nanotechnology Initiative. Nanotechnology: Big Things from a Tiny World. <https://www.nano.gov/big-things-from-a-tiny-world> (accessed 2021-02-19).
- (2) Hemminger, J. C.; Sarrao, J.; Crabtree, G.; Flemming, G.; Ratner, M. *Challenges at the Frontiers of Matter and Energy: Transformative Opportunities for Discovery Science*; U.S. Department of Energy, Office of Scientific and Technical Information: Oak Ridge, TN, 2015. <https://www.osti.gov/biblio/1283188-challenges-frontiers-matter-energy-transformative-opportunities-discovery-science> (accessed 2021-02-19).
- (3) The Office of Basic Energy Sciences. The Scale of Things Chart. 05-26-06 ed.; U.S. Department of Energy, Office of Science: <https://science.osti.gov/bes/Community-Resources/Scale-of-Things-Chart> (accessed 2021-02-19).
- (4) Blonder, R.; Joselevich, E.; Cohen, S. R. Atomic Force Microscopy: Opening the Teaching Laboratory to the Nanoworld. *J. Chem. Educ.* **2010**, *87* (12), 1290–1293.
- (5) Cross Cutting Concepts. <https://ngss.nsta.org/CrosscuttingConceptsFull.aspx> (accessed 2021-02-19).
- (6) James Gentile, K. B. *Amy Stephens Undergraduate Research Experiences for STEM Students: Successes, Challenges, and Opportunities*; National Academies of Sciences, Engineering, and Medicine: Washington DC, 2017.
- (7) Harsh, J. A. Designing performance-based measures to assess the scientific thinking skills of chemistry undergraduate researchers. *Chem. Educ. Res. Pract.* **2016**, *17* (4), 808–817.
- (8) Russell, J. E.; D'Costa, A. R.; Runck, C.; Barnes, D. W.; Barrera, A. L.; Hurst-Kennedy, J.; Sudduth, E. B.; Quinlan, E. L.; Schlueter, M. Bridging the Undergraduate Curriculum Using an Integrated Course-Embedded Undergraduate Research Experience (ICURE). *CBE-Life Sci. Educ.* **2015**, *14* (1), ar4.
- (9) Zhong, C. J.; Han, L.; Maye, M. M.; Luo, A.; Kariuki, N. N.; Jones, W. E. Atomic scale imaging: A hands-on scanning probe microscopy laboratory for undergraduates. *J. Chem. Educ.* **2003**, *80* (2), 194–197.
- (10) Maye, M. M.; Luo, J.; Han, L.; Zhong, C. J. Chemical analysis using scanning force microscopy - An undergraduate laboratory experiment. *J. Chem. Educ.* **2002**, *79* (2), 207–210.
- (11) Ashkenaz, D. E.; Hall, W. P.; Haynes, C. L.; Hicks, E. M.; McFarland, A. D.; Sherry, L. J.; Stuart, D. A.; Wheeler, K. E.; Yonzon, C. R.; Zhao, J.; Godwin, H. A.; Van Duyne, R. P. Coffee Cup Atomic Force Microscopy. *J. Chem. Educ.* **2010**, *87* (3), 306–307.
- (12) Ferguson, M. A.; Kozlowski, J. J. Using AFM Force Curves To Explore Properties of Elastomers. *J. Chem. Educ.* **2013**, *90* (3), 364–367.
- (13) Basu-Dutt, S.; Minus, M. L.; Jain, R.; Nepal, D.; Kumar, S. Chemistry of Carbon Nanotubes for Everyone. *J. Chem. Educ.* **2012**, *89* (2), 221–229.
- (14) Mackus, A. J. M.; Merkx, M. J. M.; Kessels, W. M. M. From the Bottom-Up: Toward Area-Selective Atomic Layer Deposition with High Selectivity. *Chem. Mater.* **2019**, *31* (1), 2–12.
- (15) Richey, N. E.; de Paula, C.; Bent, S. F. Understanding chemical and physical mechanisms in atomic layer deposition. *J. Chem. Phys.* **2020**, *152* (4), 040902.
- (16) *Realizing the Promise of Carbon Nanotubes*; National Nanotechnology Initiative: Arlington, VA, 2014.
- (17) Dreyer, D. R.; Park, S.; Bielawski, C. W.; Ruoff, R. S. The chemistry of graphene oxide. *Chem. Soc. Rev.* **2010**, *39* (1), 228–240.
- (18) Novoselov, K. S.; Fal'ko, V. I.; Colombo, L.; Gellert, P. R.; Schwab, M. G.; Kim, K. A roadmap for graphene. *Nature* **2012**, *490* (7419), 192–200.
- (19) Meunier, V.; Souza, A. G.; Barros, E. B.; Dresselhaus, M. S. Physical properties of low-dimensional sp(2)-based carbon nanostructures. *Rev. Mod. Phys.* **2016**, *88* (2), 025005.
- (20) Cappella, B.; Dietler, G. Force-distance curves by atomic force microscopy. *Surf. Sci. Rep.* **1999**, *34* (1–3), 5–104.
- (21) Ashraf, A.; Wu, Y. B.; Wang, M. C.; Aluru, N. R.; Dastgheib, S. A.; Nam, S. Spectroscopic Investigation of the Wettability of Multilayer Graphene Using Highly Ordered Pyrolytic Graphite as a Model Material. *Langmuir* **2014**, *30* (43), 12827–12836.
- (22) Trought, M.; Wentworth, I.; de Alwis, C.; Leftwich, T. R.; Perrine, K. A. Influence of surface etching and oxidation on the morphological growth of Al_2O_3 by ALD. *Surf. Sci.* **2019**, *690*, 121479.
- (23) Trought, M.; Wentworth, I.; Leftwich, T. R.; Perrine, K. A. Effects of Wet Chemical Oxidation on Surface Functionalization and Morphology of Highly Oriented Pyrolytic Graphite. *ChemRxiv Preprint* **2020**, No. 12907604, DOI: [10.26434/chemrxiv.12907604.v1](https://doi.org/10.26434/chemrxiv.12907604.v1).
- (24) Boulegliimat, E.; Davies, P. R.; Davies, R. J.; Howarth, R.; Kulhavy, J.; Morgan, D. J. The effect of acid treatment on the surface chemistry and topography of graphite. *Carbon* **2013**, *61*, 124–133.
- (25) Shin, Y. R.; Jung, S. M.; Jeon, I. Y.; Baek, J. B. The oxidation mechanism of highly ordered pyrolytic graphite in a nitric acid/sulfuric acid mixture. *Carbon* **2013**, *52*, 493–498.
- (26) Burgess, R.; Buono, C.; Davies, P. R.; Davies, R. J.; Legge, T.; Lai, A.; Lewis, R.; Morgan, D. J.; Robinson, N.; Willock, D. J. The functionalisation of graphite surfaces with nitric acid: Identification of functional groups and their effects on gold deposition. *J. Catal.* **2015**, *323*, 10–18.
- (27) Buono, C.; Davies, P. R.; Davies, R. J.; Jones, T.; Kulhavy, J.; Lewis, R.; Morgan, D. J.; Robinson, N.; Willock, D. J. Spectroscopic and atomic force studies of the functionalisation of carbon surfaces: new insights into the role of the surface topography and specific chemical states. *Faraday Discuss.* **2014**, *173*, 257–272.
- (28) Jang, J.; Sung, J.; Schatz, G. C. Influence of surface roughness on the pull-off force in atomic force microscopy. *J. Phys. Chem. C* **2007**, *111* (12), 4648–4654.
- (29) Burgess, R.; Buono, C.; Davies, P. R.; Davies, R. J.; Legge, T.; Lai, A.; Lewis, R.; Morgan, D. J.; Robinson, N.; Willock, D. J. The functionalisation of graphite surfaces with nitric acid: Identification of

functional groups and their effects on gold deposition. *J. Catal.* **2015**, *323*, 10–18.

(30) Guo, N.; Yam, K. M.; Zhang, C. Substrate engineering of graphene reactivity: towards high-performance graphene-based catalysts. *NPJ. 2d Mater. Appl.* **2018**, *2*, 0046–y.

(31) Thissen, N. F. W.; Vervuurt, R. H. J.; Mackus, A. J. M.; Mulders, J. L.; Weber, J. W.; Kessels, W. M. M.; Bol, A. A. Graphene devices with bottom-up contacts by area-selective atomic layer deposition. *2d Mater.* **2017**, *4* (2), 025046.

(32) Binnig, G.; Quate, C. F.; Gerber, C. Atomic Force Microscope. *Phys. Rev. Lett.* **1986**, *56* (9), 930–933.

(33) Miller, J. D.; Veeramasuneni, S.; Drelich, J.; Yalamanchili, M. R.; Yamauchi, G. Effect of roughness as determined by atomic force microscopy on the wetting properties of PTFE thin films. *Polym. Eng. Sci.* **1996**, *36* (14), 1849–1855.

(34) Zhong, Q.; Inniss, D.; Kjoller, K.; Elings, V. B. Fractured Polymer Silica Fiber Surface Studied by Tapping Mode Atomic Force Microscopy. *Surf. Sci.* **1993**, *290* (1–2), L688–L692.

(35) Burnham, N. A.; Colton, R. J. Measuring the Nanomechanical Properties and Surface Forces of Materials Using an Atomic Force Microscope. *J. Vac. Sci. Technol., A* **1989**, *7* (4), 2906–2913.

(36) Heinz, W. F.; Hoh, J. H. Spatially resolved force spectroscopy of biological surfaces using the atomic force microscope. *Trends Biotechnol.* **1999**, *17* (4), 143–150.

(37) Jang, J. Y.; Ratner, M. A.; Schatz, G. C. Atomic-scale roughness effect on capillary force in atomic force microscopy. *J. Phys. Chem. B* **2006**, *110* (2), 659–662.

(38) Hoh, J. H.; Cleveland, J. P.; Prater, C. B.; Revel, J. P.; Hansma, P. K. Quantized Adhesion Detected with the Atomic Force Microscope. *J. Am. Chem. Soc.* **1992**, *114* (12), 4917–4918.

(39) Jang, J.; Schatz, G. C. Lattice Gas Monte Carlo Simulation of Capillary Forces in Atomic Force Microscopy. *J. Adhes. Sci. Technol.* **2010**, *24* (15–16), 2429–2451.

(40) Heinz, W. F.; Hoh, J. H. Getting physical with your chemistry: Mechanically investigating local structure and properties of surfaces with the atomic force microscope. *J. Chem. Educ.* **2005**, *82* (5), 695–703.

(41) Seo, Y.; Jhe, W. Atomic force microscopy and spectroscopy. *Rep. Prog. Phys.* **2008**, *71* (1), 016101.

(42) Sedin, D. L.; Rowlen, K. L. Adhesion forces measured by atomic force microscopy in humid air. *Anal. Chem.* **2000**, *72* (10), 2183–2189.

(43) Sader, J. E.; Borgani, R.; Gibson, C. T.; Haviland, D. B.; Higgins, M. J.; Kilpatrick, J. I.; Lu, J. N.; Mulvaney, P.; Shearer, C. J.; Slattery, A. D.; Thoren, P. A.; Tran, J.; Zhang, H. Y.; Zhang, H. R.; Zheng, T. A virtual instrument to standardise the calibration of atomic force microscope cantilevers. *Rev. Sci. Instrum.* **2016**, *87* (9), 093711.

(44) Sader, J. E.; Pacifico, J.; Green, C. P.; Mulvaney, P. General scaling law for stiffness measurement of small bodies with applications to the atomic force microscope. *J. Appl. Phys.* **2005**, *97* (12), 124903.

(45) Hutter, J. L.; Bechhoefer, J. Calibration of Atomic Force Microscope Tips (VOL 64, PG 1868, 1993). *Rev. Sci. Instrum.* **1993**, *64* (11), 3342–3342.

(46) Shin, Y.-R.; Jung, S.-M.; Jeon, I.-Y.; Baek, J.-B. The oxidation mechanism of highly ordered pyrolytic graphite in a nitric acid/sulfuric acid mixture. *Carbon* **2013**, *52*, 493–498.

(47) Li, J. L.; Kudin, K. N.; McAllister, M. J.; Prud'Homme, R. K.; Aksay, I. A.; Car, R. Oxygen-driven unzipping of graphitic materials. *Phys. Rev. Lett.* **2006**, *96* (17), 176101.

(48) Marcano, D. C.; Kosynkin, D. V.; Berlin, J. M.; Sinitskii, A.; Sun, Z. Z.; Slesarev, A.; Alemany, L. B.; Lu, W.; Tour, J. M. Improved Synthesis of Graphene Oxide. *ACS Nano* **2010**, *4* (8), 4806–4814.

(49) Pourzand, H.; Tabib-Azar, M. Graphene thickness dependent adhesion force and its correlation to surface roughness. *Appl. Phys. Lett.* **2014**, *104* (17), 171603.

(50) Ding, Y. H.; Zhang, P.; Ren, H. M.; Zhuo, Q.; Yang, Z. M.; Jiang, X.; Jiang, Y. Surface adhesion properties of graphene and graphene oxide studied by colloid-probe atomic force microscopy. *Appl. Surf. Sci.* **2011**, *258* (3), 1077–1081.

(51) Butt, H. J.; Cappella, B.; Kappl, M. Force measurements with the atomic force microscope: Technique, interpretation and applications. *Surf. Sci. Rep.* **2005**, *59* (1–6), 1–152.

(52) Lai, T. M.; Meng, Y. G.; Huang, P. Adhesion forces between a parabolic-shaped AFM tip scanning a grooved gold surface: Comparison of a model and an experiment. *Int. J. Adhes. Adhes.* **2018**, *86*, 73–83.

(53) Birleanu, C.; Pustan, M.; Merie, V.; Müller, R.; Voicu, R.; Baracu, A.; Craciun, S. Temperature effect on the mechanical properties of gold nano films with different thickness. *IOP Conf. Ser.: Mater. Sci. Eng.* **2016**, *147*, 012021.